Electrical and Optical Propeties of a UV-Sensitive CCD Imager

Man-Ho Kim* and Jae-Ha Choi†

Abstract – This paper describes several improved characterizations of the EPIC CCD, which now has modified electrode and channel structures. From a 3-D numerical simulation of the device, its channel doping and potential distributions are then observed for the optimization of the charge transfer. A wavelength-dependence on the device structure is observed in terms of the reflectivity of the incident radiation. The optical properties of ultra-low energy levels, when using an open-electrode structure, are then considered to improve their quantum efficiency.

Keywords : Charge transfer efficiency, Open-electrode CCD, Qantum efficiency, UV-sensitive CCD

z1. Introduction

Charge-coupled devices (CCDs) are, at present, the most widely used major optical sensors for observing faint astronomical objects. Owing to advanced technology in the areas of read noise and charge transfer efficiency, modern scientific CCDs as focal plane detectors could have tremendously large formats with more than 4096×4096 pixels (7.5-micron pixel sensor). One of the largest single CCD array sizes has been developed by Ford/Loral Laboratories [1]. Furthermore, this could be enhanced by using a mosaic technique in order to expand the field of view. However, most of the scientific CCDs involve two major limitations: a low sensitivity at short wavelengths such as ultraviolet (UV), extreme-ultraviolet (XUV), and low energy X-ray below 1 keV, and an insufficiently low readout noise for the ultra-low signal applications (i.e. for a photon-counting detector). The former occurs due to the absorption loss in the poly-silicon electrodes and gate oxide layer as a dead layer. A back-illuminated device may be used to improve this and is, at present, under investigation at JPL (Jet-Propulsion Laboratory), Ford/Loral Laboratories, EEV, and Tektronix.

The realization of such a sophisticated structure is quite difficult. An open-electrode structure, which is easier to manufacture, is used in order to improve the sensitivity of the short wavelengths mentioned above. The read noise (at the short wavelengths) is largely dependent on the design of the output transistor and diffusion node for the charge detection. Thus, both factors should be carefully considered to achieve state-of-the-art CCDs.

In this paper, a novel open-electrode CCD device is studied for its electrical characteristics and its optical properties of ultra-low energy levels. For its characterizing investigation, a three-dimensional numerical simulation is performed to observe the potential and electron distributions. A wavelength-dependence on the device structure is observed in terms of the reflectivity of the incident radiation. The optical properties of ultra-low energy levels, when using an open-electrode structure, are then considered to improve their quantum efficiency (Q.E.).

† Corresponding Author: School of Electrical Engineering, University of Ulsan, Korea (jhchoi@mail.ulsan.ac.kr)
* School of Electrical Engineering, University of Ulsan, Korea (jamesmhkim@mail.ulsan.ac.kr)
Received 25 April 2007 ; Accepted 5 August 2007

2. Open-Electrode CCD Image Sensor

2.1. Device structure and operation

A novel open-electrode CCD sensor was fabricated by EEV Ltd. for the detection of low signal levels such as EUV, Us, and soft X-rays below 1 keV in astronomy. The structure of each pixel element consists of two different parts: one is the clocked regions and the other is the open-area regions. The buried channel region that is overlying the p-type substrate was implanted by phosphorous at approximately 1.9×10^{12} cm^{-2}. An additional shallow buried channel layer is formed beneath the 3 poly electrodes present in the open-areas. A boron implant is then installed in the open areas to achieve a surface- pinned condition. A high resistivity substrate with doping of 2×10^{12} cm^{-3} (6.5 kΩcm) is used for a deep depletion.

The structure of open-electrode CCD pixel elements is shown in Fig. 1, where the plan view, front and end elevations of the elements are given. The front and end elevations were taken from the lines A-B (along the channel-width direction) and B-D (along the charge-transfer direction),respectively. In this structure, the clocked phases are designated as phase 1 (or p1) and phase 2 (or p2),

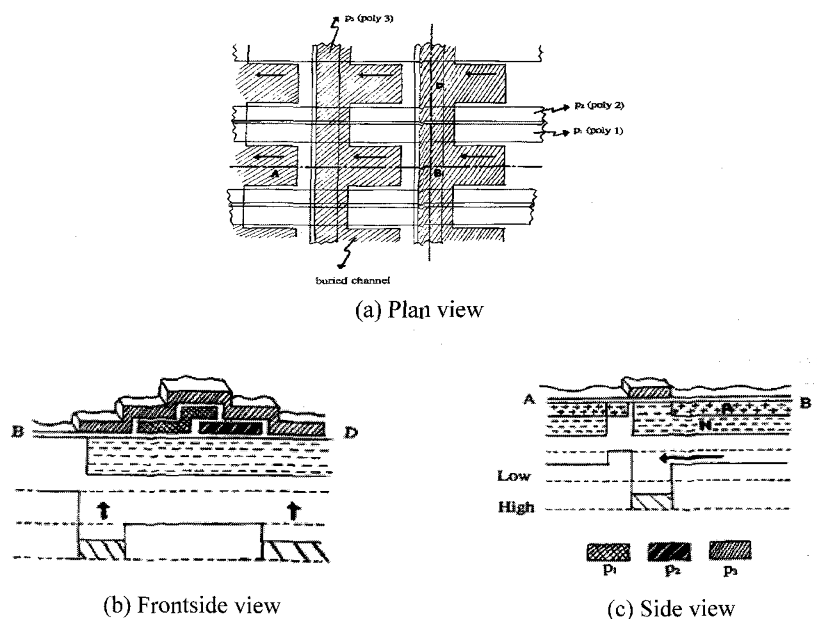

(a) Plan view

(b) Frontside view

(c) Side view

Fig. 1. The pixel structure of an open-electrode CCD.

while the phase 3 is given by phase 3 (or p3). It is seen from Fig. 1(b) and (c) that the buried channel dose exists below the three phases and the additional implanted boron impurity distribution only exists just below the open-area. During the integration time phase 1 and phase 2 are low clock voltage levels and phase 3 stays high to force the signal charge to be stored in phase 3. The potential under the open region is lower than that under phase 1 and phase 2 at low clock level, as shown in Fig 1(c). This is because the boron implant reduces the net buried channel dose in the open area, resulting in a reduction of the depletion depth [2, 3]. When phase 1 is clocked to a high level and phase 2 still remains unchanged, the charge transfer is performed from phase 3 to phase 1. In similar manner, as in the normal 3-phase CCD, subsequent charge transfer operations will be carried out by manipulating the clock pulse of each electrode.

2.2 Device description

An advanced technology of open-electrode structure opens up the era of a novel astronomical CCD for the detection of short wavelengths such as EUV, W, and soft X-rays below 1 keV. This technique combines the significant features of the current CCD devices called virtual-mode and inverted-mode CCDs, which have been widely used in astronomy. The three-phase CCDs have been developed by GEC/EEV Company for the European Photon Imaging Camera (EPIC) which will be employed for the ESA (European Space Agency) X-ray Multi-Mirror Mission (XMM) project. When an incident radiation with low energy passes through the pixel element, a low signal charge is generated in the buried channel, which corresponds to the incident photon energy. In practice, however, it is not possible for all the incident photons to penetrate the pixel element of the front-illuminated image sensor when EUV, UV, and soft X-rays below 1 keV are used.

The charge loss mainly occurs due to the dead layer which is overlying the silicon. This results in a low Q.E. device. The primary purpose of using the open-electrode device is to improve the quantum efficiency for the energy band mentioned above, increasing its sensitivity. This can be achieved with the pixel including a free of polysilicon area that is being used in the back-illuminated CCDs for a good spectral response of the short wavelengths. This modified electrode structure allows a high charge generation below the open area. An important feature of the device is that a reduction in dark current is possible by reducing the effective channel area since the dark current contribution is proportional to the channel area covered by the polysilicon electrode when the device is irradiated by protons (during the satellite missions in space). The dark current source, due to traps formed by the radiation damage, results in a reduced charge transfer efficiency and thus energy resolution since interactions of signal charge with the traps occur during the charge transfer [4]. Thus, an enhanced radiation tolerance of the device can be achieved by narrow supplementary buried channel implantations (or notches), as demonstrated by Janesick et. al [5]. They demonstrated the effects of radiation damage

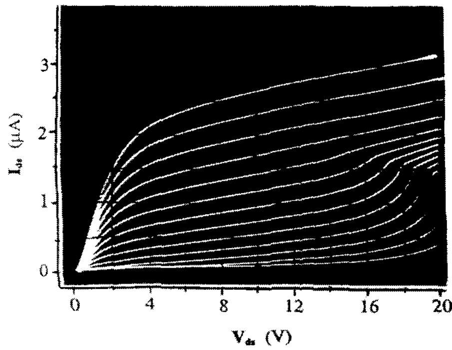

Fig. 2. I-V Charateristic curves of a buried channel MOSFET.

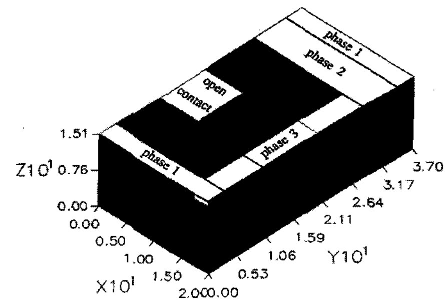

Fig. 3. A 3-D device structure, of an open-electrode CCD, used for the simulation.

encountered by protons and presented a suppression method of the proton-induced displacement damage by using a notch technique.

The open-electrode device incorporated a narrow heavily doped channel region of 3.5 μm in which a higher maximum potential exists than the normal channel potential. A p^+ - implant is

necessary under the open-area for several reasons. The reasons for this are a surface dark current suppression due to the open surface pinned to substrate potential and a higher charge transfer efficiency which is achieved by preventing the signal charge from back-spilling under the phase 1 or phase 2 into the open regions during the vertical charge transfer.

For a higher Q.E., the pixel structure should have a thinner gate oxide layer in the open-electrode area since a low signal, corresponding to several hundred electrons, may be affected by the layer. As an example, to detect Carbon k X-ray photons of 300 eV, one probably needs a CCD device with a p^+-open surface thickness of <100 nm since the corresponding absorption length does not exert a strong influence on the optical charge generation above this region [3]. Thus, to detect such low energy levels of XUV and UV and soft x-ray below 1 keV with satisfactory sensitivity one alternative way is to minimize the gate oxide layer and to use thinner poly gates within the clocked regions for reducing interference fringing effect [3]. An important feature is that during the line readout in horizontal registers the vertical clocks should make all surfaces inverted to improve the CTE. This open-electrode CCD has a similar mode to normal 3-phase CCDs except that the open-area in each pixel is only included in the vertical register.

2.3 Device simulation

During this work, many different device simulations have been performed to demonstrate an analysis technique for a deep depletion BC MOSFET and BC CCD. A transistor curve tracer can be used to produce sets of

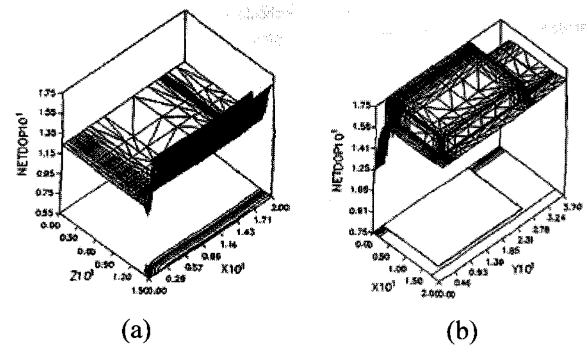

(a) (b)

Fig. 4. 3-D isometric channel net-doping distributions and their contours extracted (a) on the Si-SiO_2 surface interface and (b) in the centre of phase 3. The magnitude of the doping concentration is given as LOC (N_A-N_D).

operational chara-cteristic curves of MOSFETs. The I-V charac-teristic curves of a typical CCD MOS transistor fabricated by EEV Ltd. are shown in Figure 2. These curves were obtained with a substrate bias of -10 V, varying gate-to-source voltages from 0 V to -12 V (in which a vertical scale of I_D=0.5μA/div and horizontal scale of V_{ds}=2V/div was given). It is shown from the curves that avalanche breakdown caused by an impact ionization occurs at V_{ds}>18 V.

The device structure of an open-electrode CCD pixel element was simulated in three dimensions; this is shown in Fig. 3. In this simulation, only half of the analysis domain was modeled due to its symmetrical doping structure (with respect to the centre of a phase 3) along the channel-width direction. An open-pin contact is used for pinning the open-surface to the substrate. An oxide thickness of 85 nm was used for this simulation. In this simulation, only half of the analysis domain was modeled due to its symmetrical doping structure (with respect to the centre of a phase 3) along the channel-width direction. An open-pin contact is used for pinning the open-surface to the substrate. An oxide thickness of 85 nm was used for this simulation. It should be noted that a cross-linked poly 3 electrode was employed to avoid the connection problem[2].

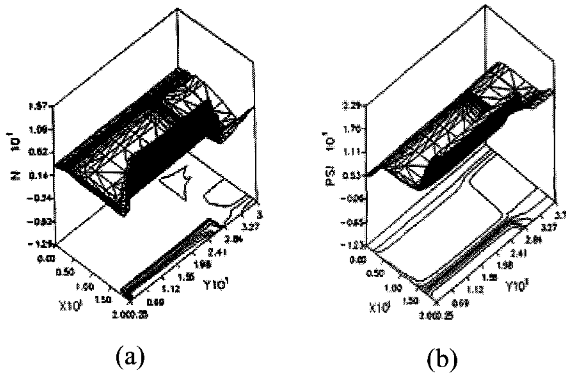

Fig. 5. 3-D isometric potential (a) and electron (b) distributions extracted on a potential minimum.

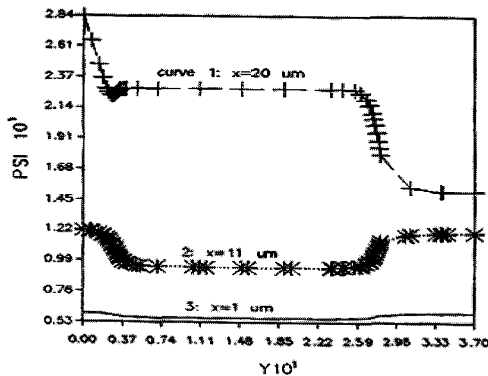

Fig. 6. The corresponding potentials (along the channel-transfer direction), of Fig. 5a. extracted from the centers of a supplementary channel width (at x=20 μm), a buried channel width (at x=11 μm), and a column isolation region (at x=1 μm).

Three-dimensional (3-D) channel net-doping distributions and their contours extracted on the Si/Si02 surface interface and in the centre of the phase 3 are isometrically shown in Fig. 4a and 4b, respectively.

The magnitude of the doping concentration is given as LOG (N_A-N_D). It is seen from Fig. 4a that a highly-doped acceptor impurity exists across the open-area. A buried-channel doping (including the acceptor impurity) distribution underneath the open-area and a supplementary buried-channel doping distribution underneath phase 3 are indicated in Fig. 4b. The 3-D potential and electron distributions on a potential minimum (at 0.5 μm away from the surface) were found, as presented in Fig. 5. In Fig. 5b the magnitude of the electron distribution is given on a LOG scale. From Fig. 5 it can be demonstrated that the supplementary channel doping allows charge storage due to a sufficiently high potential minimum under phase 3 with respect to the potentials under phases 1 and 2.

This can be seen from Fig. 6 where the corresponding potential curves (along the channel-transfer direction of Fig. 5a) are plotted. They are extracted from the centers of a supplementary channel width, a buried channel width, and a column isolation region.

The potential difference between the two channels was then found to be 13.8 V. For this analysis, phases 1, 2, and 3 are biased to 0, 0 and 10 V, respectively and a flat band voltage is 0 V. This 3-D simulation was done using a 3-D device simulator, "EVEREST", [6] which has been demonstrated at the previous work for the characterizing analysis of a JET-X CCD [7, 8].

They are extracted from the centers of a supplementary channel width, a buried channel width, and a column isolation region. The potential difference between the two channels was then found to be 13.8 V. For this analysis phases 1, 2, and 3 are biased to 0, 0 and 10 V, respectively and the flat band voltage is 0 V.

3. UV wavelength dependence of the opto-electrical conversion

3.1. Optical properties of the air-SiO2-Si structure

The optical properties of the air- SiO_2-Si structure are, in general, determined by the absorption coefficient and its index of refraction. The wavelength dependence encountered by the incident photons is that of the reflection due to the interference between the transmitted optical radiation at the air-SiO_2 interface and the radiation reflected at the SiO_2-Si interface. The optical sensitivity of the interfaces largely depends on the thickness of the oxide layer relative to the wavelength in the part of the spectrum under consideration. Furthermore, the reflection coefficient at the SiO_2-Si interface is coupled to the absorption coefficient through the index of refraction and the extinction coefficient in the silicon. The photons that are transmitted through the SiO_2layer into the silicon are able to generate electron-hole pairs. The charge collection efficiency can then be defined as the average number of electron-hole pairs generated from the absorption of one photon in the semiconductor. For incident photon energy, hv, being much larger than a bandgap energy, E_g, transition probability increases with the energy of the incident photons. This transition from the top of the valence band to the bottom of the conduction band occurs due to the reduction of the required momentum, increasing the absorption coefficient. The absorption coefficient, u, for the medium is a measure of the amount of the incident radiant energy absorbed, at normal incidence, through a unit distance or by a unit mass of absorbing medium and is given by:

$$\alpha = \frac{2wK}{c} = \frac{4\pi K}{\lambda} \quad (1)$$

where λ is the wavelength of the incident radiation, w is the angle frequency, c is the light velocity, and K is the absorption index.

The reflection and transmission coefficients are real quantities defined by the ratios of the energy flows in the reflected and refracted waves with respect to the incident wave. Since there is a requirement for energy to be conserved at the interface, the transmission coefficient, T, is given by T = 1 - R, where R is reflectivity. For an open-electrode structure with an air-SiO_2-Si system, at normal incidence, the reflectivity and the transmission coefficient on an interface between the first medium of air with a refractive being 1 and the second medium of silicon with a complex refractive are given by

$$R = \{\frac{n(\lambda) - iK(\lambda) - 1}{n(\lambda) - iK(\lambda) + 1}\}^2 = \frac{(n(\lambda)-1)^2 + K^2(\lambda)}{(n(\lambda)+1)^2 + K^2(\lambda)} \quad (2)$$

and

$$T = \frac{4\{n(\lambda) - iK(\lambda)\}}{\{n(\lambda) - iK(\lambda) + 1\}^2} = \frac{4\{n(\lambda) - iK(\lambda)\}}{(n(\lambda)+1)^2 + K^2(\lambda)} \quad (3)$$

where n and K are real index and imaginary (or absorption) parts of the refractive index for silicon. The wavelength dependence of the reflection shows that the interference between the incident radiation and the multiple reflected radiation in the oxide and wavelength dependence of the refractive index in silicon exists. A better expression for the reflection at normal incidence with an air-SiO_2-Si structure may be given by

$$R = \frac{(A\cos\phi + B)^2 + (C\sin\phi - D)^2}{\{(A+2)\cos\phi - B\}^2 + \{(C+2n1)\sin\phi + D\}^2} \quad (4)$$

with $A = n2(\lambda) - 1$,

$B = \{K2(\lambda)/n1\}\sin\phi$

$C = \{n2(\lambda)/n1\} - n1$,

$D = K2(\lambda)\cos\phi$

and $\phi = (2\pi/\lambda)n1x_{ox}\cos\theta$

where n1 is the real Part of the refractive index for SiO_2, n2 and K2 are the real and imaginary parts of the refractive index for Si, x_{ox} is an oxide thickness, and θ is the angle of refraction. This theoretical calculation is only valid provided that the oxide layer has only a real index of refraction equal to n1=1.46, which means it has no absorption through the oxide thickness i.e. zero absorption index.

3.2. Considerations for determination of Quantum Efficiency in an open-electrode structure

For photons with a long absorption length (i.e. wavelengths less than 1 nm or greater than 600 nm), the Q.E. depends largely on the thickness of the photosensitive volume. Intermediate wavelengths have relatively short absorption lengths in silicon and SiO_2, and throughout this spectral region the Q.E. depends largely on the transparency, reflectance, and surface conditions of the surface layers that overlie the photosensitive volume. For $\lambda < 180$ nm, most of the incident radiation energy is lost in the gate electrode and the SiO_2 layer, resulting in a sudden decrease of Q.E.. For $\lambda > 650$ nm, the Q.E. becomes very poor due to the long penetration in the substrate since most of the charge carriers generated in the substrate have a high probability of recombination due to their short lifetime. In this case the improvement of Q.E. is achieved by using a thicker device and a high-purity starting material for the deep depletion CCD. Most scientific CCDs used for UV or XUV detection in astronomy have a very poor Q.E. due to high absorption loss since the absorbing depth of UV photons is short enough to stay in the dead layer. An open-electrode CCD device without a polysilicon electrode is necessary to avoid this problem. Measurements of quantum efficiencies of an open-electrode sensor were performed using a DTF (Detector Test facility) system set on XUV exposure using Neon wavelengths such as 16 nm (77.5 eV), 46.1 nm (26.9 eV), and 73.5 nm (6.9 eV). It was found from the measurement that the measured Q.E. was less than 1%. It is believed that the poor Q.E. resulted primarily from the factors listed below;

a. Due to the poor quartz filter
b. Due to the dead layer corresponding to the oxide thickness
c. Due to the higher reflectivity based on the optical properties of Neon wavelengths in an air-SiO_2-Si system.
d. Due to the increase of Si/SiO_2 interface surface states cause by radiation damage.
e. Due to the partial events which may result in small signal loss.

To measure an XUV signal, a differencing signal is taken by subtracting a signal penetrated through a quartz filter from a signal penetrated without it. For an open electrode structure the oxide thickness of 85 m as a dead layer is used since a thin layer of silicon dioxide is required to passivate the exposed surface. The absorption coefficient of SiO_2 is slightly larger than that of silicon. The reflectivity for the air-SiO_2-Si structure was

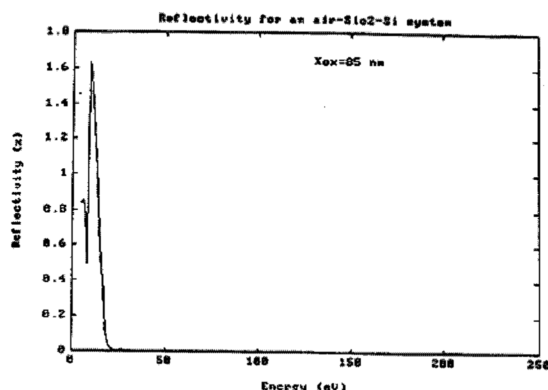

Fig. 7. Reflectivity for an oxide thickness of 85 nm the in air- SiO_2-Si structure of an open-electrode area.

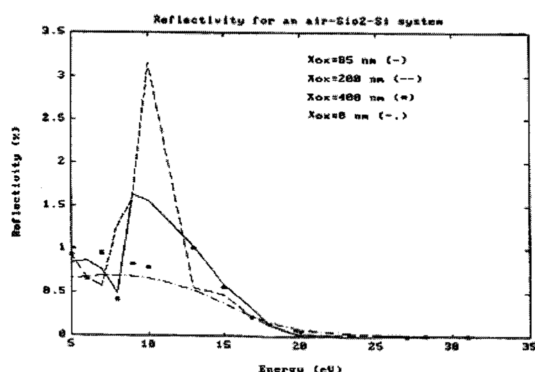

Fig. 8. Reflectivities for four different oxide thickness in an air- SiO_2-Si structure or an open-electrode area.

calculated using Equation 4 for the energy band ranging from 0 to 250 eV, as shown in Fig. 7, which is almost constant and negligibly low for the energy range used, except at 10 eV. The peak value at 10 eV is due to the higher dielectric constant for the oxide layer. Reflectivities for four different thick layers of SiO_2 are also shown in Fig. 8 It is demonstrated from Fig. 8 that the variation of oxide thickness has no significant influence on reflectivity but a minimum reflectivity can be achieved with no oxide layer. The calculated results were obtained under the assumption that in Equation 4 the oxide layer is thin enough and thus the absorption coefficient of the SiO_2 is negligible. A better approximation to the reflectivity can be achieved when the absorption coefficient of the SiO_2 is considered in Equation 4. It is suggested that for the improvement of Q.E. of the device, the oxide thickness as a dead layer should be further reduced, if possible.

4. Acknowledgements

This work was supported by the 2007 Research Fund of the University of Ulsan.

5. Conclusions

We have investigated the optical properties of short wavelengths such as UV, XUV, and low-energy X-rays below 1 keV and their wavelength-dependence on a CCD electrode structure. Poor sensitivity of the detection of such low-energy levels in CCDs resulted from a dead layer present above the photo-sensitive volume. A higher sensitivity (or Q.E.) can be achieved by reducing a gate oxide layer in an open-phase and using thinner poly gates within the clocked-phases and a light filter (rather than a quartz filter) for an open-electrode CCD structure. For an open-electrode CCD an enhanced sensitivity is possible since the pixel element includes a clocking phase with an open-electrode area. An additional boron implantation below an open-phase provides a surface dark current suppression by pinning a surface of the open-area to the substrate as well as no back-spilling of the charge signal stored under each open-phase. Narrow supplementary buried channel implantations (or notches) were performed to ensure a high radiation tolerance of the device, resulting in a reduction of the probability of the radiation-induced traps and thus improved CTE and energy resolution.

References

[1] J. Janesick, T. Elliott, A. Dingizian, R. Bredthauer, C. Chandler, J. Westphal and J. Gunn, "New advancements in charge-coupled device technology-sub-electron noise and 4096×4096 pixel CCDs", Proc. SPIE, v. 1242, (1990).

[2] D.J. Burt, EEV Confidential Report, 1992.

[3] J. Janesick, "Open pinned-pahse CCD technology", Proc. SPIE, v. 1159, (1989).

[4] A.D. Holland, "Radiation effects in CCD X-ray detectors," Ph.D. thesis, Leicester University, (1990).

[5] J. Janesick, G. Soli and S. Cllins, "The effects of proton damage on Charge-Coupled Devices". Proc. SPIE, v.1447, p.87, (1991).

[6] C. Greenough, "Three dimensional algorithms for a robust and efficient semiconductor simulator with parameter extraction: The EV-EREST final report", Project Report (1992).

[7] M.H. Kim, Determination of the depletion depth of the deep depletion charge-coupled devices, Journal of Electrical Engineering & Technology, vol. 1. No. 2, p. 233, (2006).

[8] M.H. Kim, 3-dimensional numerical analysis of deep depletion buried channel MOSFETs and CCDs, Journal of Electrical Engineering & Technology, vol . 1. No. 3, p. 396, (2006).

Man-Ho Kim
He received his Ir degree from Delft University of Technology in Holland (1986-1989) and his Ph.D. from Leicester University in the UK (1992-1995). His research interests are the CCD/CMOS image sensor and the optical laser transmission system.

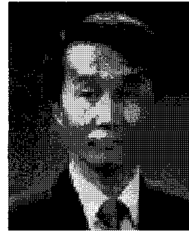

Jae-Ha Choi
He received his B.S. and M.S. degrees from Yonsei University in 1976 and 1978, respectively. Currently, he is a Professor in the School of Electrical Engineering, University of Ulsan.